Numerical investigation of thin films with strain gradient elasticity

B. Emek Abali, Wolfgang H. Müller, Victor A. Eremeyev
abali@tu-berlin.de

Abstract

Thin films are applied in Micro-Electro-Mechanical Systems (MEMS). The mechanical response of thin films on the micrometer length scale is different from their response on the macroscale. In order to model this phenomenon we propose to apply the so-called *strain gradient elasticity*. There are various versions of strain gradient theory available in the literature. After a brief review of our version, we use finite element and finite difference methods for computing the deformation state of thin films by using strain gradient elasticity. Moreover, we perform a numerical study of Cu films of different thicknesses and observe qualitatively the same phenomena as in experiments.

1 Introduction

The miniaturization of electro-mechanical systems requires producing and the use of geometries on the microscale. Nowadays, thin films applied in Micro-Electro-Mechanical Systems (MEMS) are even smaller than 1 µm. As a material for such thin films copper (Cu) is often used due to its high conductance and specific strength. The behavior of Cu on the macroscale can be modeled accurately by using the theory of elasticity. Interestingly, the mechanical response of Cu changes on the micrometer length scale. Especially for Cu thin films this phenomenon has been observed experimentally, see for example Gruber et al. (2008) and Wang et al. (2014). Such a change of the mechanical behavior is referred to as (elastic) *size effect*. The ordinary theory of elasticity fails during its characterization, consequently, it needs to be extended. In order to calculate the mechanical behavior of thin films we propose to use the so-called strain gradient elasticity instead. There have been various variants of strain gradient elasticity. For an overview see Gurtin et al. (2010, §90). We give a brief outline of our version based on rational continuum mechanics and then perform a numerical study of Cu thin films.

First, we start with the balance equations of linear and angular momenta. Their flux terms are known to be the stress tensor and the couple stress tensor for a non-polar medium, such as Cu. Second, we apply a suitable method to obtain the necessary constitutive equations for the stress and couple stress tensors. By closing the balance equations with suitable constitutive equations we obtain the field equations. Third, we employ a variational formulation for generating a weak

form of the field equations. This weak form can be evaluated computationally by using numerical solution techniques. We use the finite element method for space discretization and the finite difference method for time discretization, and then solve the weak form by using open-source packages developed under the FEniCS project, see Logg et al. (2011). Thin films made of Cu are simulated with our version of strain gradient elasticity. We perform a numerical study of different thicknesses, and observe qualitatively the same deformation phenomenon as in real experiments.

2 Governing equations

Throughout the paper we use the standard nomenclature of continuum mechanics including the summation convention for repeated indices. We consider a continuum body, $\mathcal{B}_0$, consisting of massive particles at *known* original positions X_i, expressed in Cartesian coordinates. In a material frame the particles are identified by their original positions X_i. As a consequence of (mechanical) loading the body deforms to $\mathcal{B}$ at the present time t and the particles move to $x_i = x_i(X_j, t)$. The objective of continuum mechanics is to calculate this deformation by determining the displacement of each particle:

$$u_i = u_i(X_j, t) = x_i - X_i \ . \tag{1}$$

In the theory of elasticity this is achieved by satisfying the balance of linear momentum. In strain gradient elasticity we need to fulfill also the balance of angular momentum. Both balances of momenta transformed onto the initial frame, $\mathcal{B}_0$, read

$$\begin{aligned} \rho_0 \frac{\partial v_i}{\partial t} - \frac{\partial P_{ji}}{\partial X_j} - \rho_0 f_i = 0 \ , \\ \rho_0 \frac{\partial a_{ik}}{\partial t} - \frac{\partial A_{ijk}}{\partial X_j} - \rho_0 z_{ik} = 0 \ , \end{aligned} \tag{2}$$

where the specific linear momentum (per mass), v_i, and the specific angular momentum, a_{ik}, are the unknowns. The flux terms, P_{ji} and A_{ijk}, will be defined by using constitutive equations. The supply terms, f_i and z_{ik}, are prescribed and known. For a motivation and a derivation of these balance equations from the well-known global balance equations in the current frame we refer to Abali et al. (2015). The specific linear momentum, v_i, is a tensor of rank one. Physically speaking, it is the velocity of the material particles, and given as follows in the initial frame:

$$v_i = \frac{\mathrm{d}x_i(X_j, t)}{\mathrm{d}t} = \frac{\partial x_i(X_j, t)}{\partial t} = \frac{\partial (u_i + X_i)}{\partial t} = \frac{\partial u_i}{\partial t} \ , \tag{3}$$

since the initial positions of particles are constant. The specific angular momentum, a_{ik}, is a tensor of rank two and consists of a spin and a moment of linear momentum. For non-polar materials, such as copper, the spin vanishes and a_{ij} becomes:

$$a_{ik} = X_{[i} v_{k]} = \frac{1}{2}\big(X_i v_k - X_k v_i\big) \ . \tag{4}$$

Hence, in both balances of momenta the displacement field, u_i, occurs, which is the unknown field. After vector multiplication of the balance of linear momentum by the

position vector and subsequent substraction from the balance of angular momentum we obtain the balance of spin. It contains a production term. Since the spin vanishes for a non-polar material, its production term has to vanish, too. This restriction requires the CAUCHY stress tensor, $\sigma_{ij} = \sigma_{ji}$, *i.e.*, the flux of linear momentum in the current frame, to be symmetric. The flux of linear momentum in the initial frame is referred to as the first PIOLA-KIRCHHOFF stress tensor:

$$P_{ji} = J(\boldsymbol{F}^{-1})_{jk}\sigma_{ki} \ , \quad J = \det(\boldsymbol{F}) \ , \quad F_{ij} = \frac{\partial x_i}{\partial X_j} \ . \tag{5}$$

Obviously, the first PIOLA-KIRCHHOFF stress fails to be symmetric even in case of a symmetric CAUCHY stress, σ_{ji}. Hence the second PIOLA-KIRCHHOFF is introduced:

$$S_{kj} = P_{ki}(\boldsymbol{F}^{-1})_{ji} \ , \quad S_{kj} = S_{jk} \ . \tag{6}$$

The flux of angular momentum consists of a flux of spin and a moment of flux of linear momentum:

$$A_{ijk} = \mu_{ijk} + X_{[i}P_{jk]} = \mu_{ijk} + \frac{1}{2}\big(X_iP_{jk} - X_kP_{ji}\big) \ . \tag{7}$$

The flux of spin, μ_{ijk}, is also called *couple stress* in the initial frame. We need to find constitutive equations for the stress, S_{ij}, and the couple stress, μ_{ijk}, with respect to the unknowns, *i.e.*, the displacement components, u_i. Then the following two equations lead to the displacement field:

$$\begin{aligned} \rho_0\frac{\partial^2 u_i}{\partial t^2} - \frac{\partial P_{ji}}{\partial X_j} - \rho_0 f_i = 0 \ , \\ \rho_0 X_{[i}\frac{\partial^2 u_{k]}}{\partial t^2} - \frac{\partial \mu_{ijk}}{\partial X_j} - P_{[ik]} - X_{[i}\frac{\partial P_{jk]}}{\partial X_j} - \rho_0 z_{ik} = 0 \ . \end{aligned} \tag{8}$$

The specific supply term for the linear momentum, f_i, is given by the gravitational specific force only, since we neglect electromagnetic interaction in the system. The specific supply term for the angular momentum, z_{ik}, consists of two terms, a specific body force affecting the spin volumetrically, and a moment of the gravitational specific force. Since the material is non-polar the first term is neglected, we have:

$$z_{ik} = X_{[i}f_{k]} = \frac{1}{2}\big(X_if_k - X_kf_i\big) \ . \tag{9}$$

By inserting the latter in Eq. $(8)_2$ we realize that the couple stress has the following symmetry property:

$$\mu_{ijk} = -\mu_{kji} \ . \tag{10}$$

Next, we will define the stress and the couple stress tensors depending on the displacement field. Due to objectivity we need to use the gradient of displacement. In this context we use the GREEN-LAGRANGE strain tensor:

$$E_{ij} = \frac{1}{2}\big(C_{ij} - \delta_{ij}\big) \ , \quad C_{ij} = F_{ki}F_{kj} \ . \tag{11}$$

In the theory of elasticity the stress is given by the strain, which is sufficient to determine the displacements accurately. In strain gradient theory the additional flux term, *i.e.*, the couple stress, is described by the strain gradient, $\partial E_{ij}/\partial X_k$. Theoretically stress may depend on the strain gradient as well as couple stress may depend on the strain. For linear and isotropic materials this is not the case, see dell'Isola et al. (2009, §3). Hence we can define the general *linear* relations for the stress and couple stress as follows

$$S_{ij} = C_{ijkl}E_{kl} \ , \quad \mu_{ijk} = D_{ijklmn}E_{lm,n} \ . \tag{12}$$

The so-called stiffness tensor C_{ijkl} is of rank four and the tensor D_{ijklmn} is of rank six. For isotropic materials the tensorial forms of such material tensors are well-known, see for example Suiker and Chang (2000). Since the strain is symmetric, $E_{ij} = E_{ji}$, we obtain the following stiffness tensor:

$$S_{ij} = \lambda E_{kk}\delta_{ij} + 2\mu E_{ij} \ , \tag{13}$$

where the LAMÉ parameters are given by the engineering constants, viz., YOUNG's modulus, E, and POISSON's ratio, ν, as follows:

$$\lambda = \frac{E\nu}{(1+\nu)(1-2\nu)} \ , \quad \mu = \frac{E}{2(1+\nu)} \ . \tag{14}$$

Analogously, we obtain the material tensor D_{ijklmn} after using the conditions $E_{ij,k} = E_{ji,k}$ and $\mu_{ijk} = -\mu_{kji}$, such that

$$\mu_{ijk} = \alpha\big(\delta_{ij}E_{km,m} - \delta_{jk}E_{im,m}\big) + \beta\big(\delta_{ij}E_{mm,k} - \delta_{jk}E_{mm,i}\big) + \gamma\big(E_{ij,k} - E_{jk,i}\big) \ . \tag{15}$$

The couple stress possesses three additional material parameters. After measuring E, μ, α, β, γ we can calculate the deformation of thin films. An adequate numerical implementation is presented in the following section.

3 Numerical implementation

The field equations (8) are differential equations in space and time. In order to analyze them numerically we need to discretize the fields and operators in space and time. For discretization in time we use the *finite difference method*:

$$\frac{\partial u_i}{\partial t} = \frac{u_i - u_i^0}{\Delta t} \ , \quad \Delta t = t^{(k+1)} - t^{(k)} \ , \tag{16}$$

This implicit method is stable for real valued problems. For the space discretization we employ the GALERKIN-type *finite element method*, where the test functions, δu_i, are chosen from the same SOBOLEV space as the unknowns, u_i. We use continuous second order elements belonging to

$$\begin{aligned} \mathcal{V} &= \{u_i \in [\mathcal{H}^2(\Omega)]^3 : u_i\big|_{\partial\Omega} = \text{given}\} \ , \\ \hat{\mathcal{V}} &= \{\delta u_i \in [\mathcal{H}^2(\Omega)]^3 : \delta u_i\big|_{\partial\Omega} = \text{given}\} \end{aligned} \tag{17}$$

for the three dimensional domain $\Omega \in \mathbb{R}^3$ and its boundaries $\partial\Omega$. The weak form is obtained by multiplying the field equations with appropriate test functions and then applying integration by parts:

$$\begin{aligned} \mathrm{F} = \sum_{\text{elements}} \int_{\Omega^e} \Big(& \rho_0 \frac{u_i - 2u_i^0 + u_i^{00}}{\Delta t \Delta t} \delta u_i + P_{ji} \delta u_{i,j} - \rho_0 f_i \delta u_i + \\ & + \rho_0 X_{[i} \frac{u_{k]} - 2u_{k]}^0 + u_{k]}^{00}}{\mathrm{d}t\, \mathrm{d}t} \delta u_{k,i} + \mu_{ijk} \delta u_{k,ij} - P_{[ik]} \delta u_{k,i} - X_{[i} P_{jk],j} \delta u_{k,i} - \\ & - \rho_0 l_{ik} \delta u_{k,i} - X_{[i} f_{k]} \delta u_{k,i} \Big) \, \mathrm{d}V - \int_{\partial\Omega} \big(P_{jk} \delta u_k + \mu_{ijk} \delta u_{k,i} \big) N_j \, \mathrm{d}A \; . \end{aligned} \tag{18}$$

This weak form is implemented in Python by using open-source packages developed by the FEniCS project, Logg et al. (2011). Since the weak form is nonlinear, it is linearized by a fully automatized symbolic derivative at the level of partial differential equations, see Alnaes and Mardal (2010). All 2D-plots were created by using the MatpPlotLib packages, see Hunter (2007), under NumPy, see Oliphant (2007).

4 Results and conclusion

The deformation behavior of thin films has been analyzed. We consider a plate with dimensions $10 \times 10 \times 1$ length units on the microscale. By varying the length unit, the length to thickness ratio is kept constant. The geometry remains the same, whereas the geometric scale is changing. In order to perform a somewhat realistic simulation we use the properties of High Conductivity Phosphorus Deoxidized Copper (CU-HCP). The material is modeled as isotropic with YOUNG's modulus taken as $E = 139.9\,\mathrm{GPa}$ at room temperature, see Müller et al. (2011). We assume POISSON's ratio to be $\nu = 0.3$ and take the mass density as $\rho_0 = 8960\,\mathrm{g/\mu m^3}$. The plate is subjected to tensile test conditions: On one end it is clamped by setting the displacements equal to zero. On the other end it is stretched by setting the displacement analogously to a position controlled in tensile testing. For all other boundaries free surface conditions have been implemented, such that the boundary terms vanish. During one "second" the strain is increased linearly up to 0.2% and the stress is computed at that strain. From experiments, see Gruber et al. (2008, Fig. 8), we expect approximately 300 MPa of stress at 0.2% of strain. In Fig. 1, at strain $E_{11} = 0.002$ the true stress, namely the CAUCHY stress, σ_{11}, is plotted by varying the film thickness. The so-called size effect is obvious. Although the geometric ratios and material parameters remain the same, the behavior alters by varying the thickness. Interestingly this change is not monotonous and seems to be counter-intuitive. We know from the experiments that such a behavior occurs in reality, see Gruber et al. (2008, Fig. 9c). From Gruber et al. (2008, Fig. 8) it is known that the material's response up to 0.1% is identical for different thicknesses. In Gruber et al. (2008) this discrepancy has been motivated by a possible change in plasticity without any change of the elastic response. However, it is then difficult to justify the change in the initial yield stress. In this paper we present a simulation with a qualitatively similar response of the material, where the change is explained

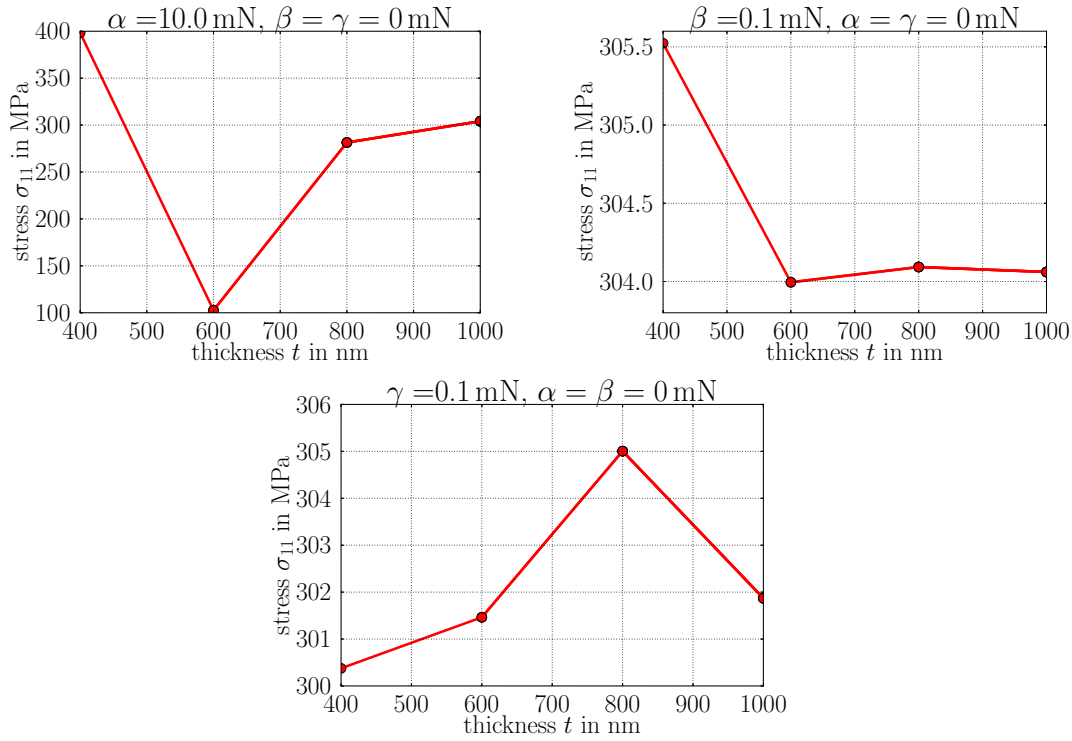

Figure 1: Variation of thickness of thin film out of Cu-HCP. The ordinate refers to the normal stress value at 0.2% of tensile strain.

by our version of strain gradient theory.

We started with a brief outline of the strain gradient theory and its implementation, which are mainly developed in Abali et al. (2015). Additional to the well-known engineering constants three more material parameters were necessary to model a system using strain gradient theory. For simulations of thin films we determined these parameters by free choice and achieved to model the counter-intuitive response of thin films. It is rather challenging to obtain qualitatively accurate results by finding the correct set of parameters.

References

Abali, B. E., Müller, W. H., and Eremeyev, V. A. 2015. Strain gradient elasticity with geometric nonlinearities and its computational evaluation. –submitted–.

Alnaes, M. S. and Mardal, K.-A. 2010. On the efficiency of symbolic computations combined with code generation for finite element methods. ACM Transactions on Mathematical Software, 37(1):6:1–6:26.

dell'Isola, F., Sciarra, G., and Vidoli, S. 2009. Generalized Hooke's law for isotropic second gradient materials. Proceedings of the Royal Society A: Mathematical, Physical and Engineering Science, 465:2177–2196.

Gruber, P. A., Böhm, J., Onuseit, F., Wanner, A., Spolenak, R., and Arzt, E. 2008. Size effects on yield strength and strain hardening for ultra-thin Cu films with and without passivation: A study by synchrotron and bulge test techniques. Acta Materialia, 56(10):2318–2335.

Gurtin, M. E., Fried, E., and Anand, L. 2010. The mechanics and thermodynamics of continua. Cambridge University Press.

Hunter, J. 2007. Matplotlib: A 2d graphics environment. Computing In Science & Engineering, 9(3):90–95.

Logg, A., Mardal, K. A., and Wells, G. N. 2011. Automated solution of differential equations by the finite element method, the FEniCS book, volume 84 of Lecture Notes in Computational Science and Engineering. Springer.

Müller, W. H., Worrack, H., and Zapara, M. 2011. Analysis of nanoindentation experiments by means of atomic force microscopy. PAMM, 11(1):413–414.

Oliphant, T. E. 2007. Python for scientific computing. Computing in Science & Engineering, 9(3):10–20.

Suiker, A. and Chang, C. 2000. Application of higher-order tensor theory for formulating enhanced continuum models. Acta mechanica, 142(1-4):223–234.

Wang, D., Gruber, P. A., Volkert, C. A., and Kraft, O. 2014. Influences of Ta passivation layers on the fatigue behavior of thin Cu films. Materials Science and Engineering: A, 610:33–38.

B. Emek Abali, Technische Universität Berlin, Institute of Mechanics, Einsteinufer 5, D-10587 Berlin, Germany

Wolfgang H. Müller, Technische Universität Berlin, Institute of Mechanics, Einsteinufer 5, D-10587 Berlin, Germany

Victor A. Eremeyev, Otto-von-Guericke-Universität Magdeburg, Institute of Mechanics, Universitätsplatz 2, D-39106 Magdeburg, Germany